3RD WORKSHOP ON MACHINE LEARNING IN NETWORKING (MaLeNe) PROCEEDINGS

SEPTEMBER 1, 2025

CO-LOCATED WITH
THE 6TH INTERNATIONAL CONFERENCE ON NETWORKED SYSTEMS (NETSYS 2025)
ILMENAU, GERMANY

Emotion-Controlled Communication in Agent Networks

1st Yanakorn Ruamsuk
Faculty of Mathematics and Computer Science
FernUniversität in Hagen
Hagen, Germany
yanakorn.ruamsuk@gmail.com

2nd Herwig Unger
Faculty of Mathematics and Computer Science
FernUniversität in Hagen
Hagen, Germany
herwig.unger@gmail.com

***Abstract*—Communication within agent networks involves multiple input and output parameters, making adaptive control and interpretation difficult. Existing systems typically rely on fixed rules or reactive behavior, lacking mechanisms for self-regulation or proactive engagement. This paper proposes an emotion-controlled communication framework, where internal emotional states act as an intermediate layer between input stimuli and output generation. Emotions are modeled using analog circuits to simulate continuous accumulation, decay, and inter-emotional feedback. Simulations with two agents—one active, one passive—demonstrate how internal states evolve in response to input and influence communication behavior over time.**

***Index Terms*—agent communication, emotion modeling, analog circuits, affective systems, internal regulation**

I. Introduction

Modern agent networks—such as those built from cooperating platform interfaces or decentralized service agents—require robust mechanisms to manage communication across multiple participants [1], [2]. These agents often operate through rule-based systems, fixed turn-taking logic, or event-driven APIs, limiting their ability to adapt, self-regulate, or behave meaningfully in dynamic environments. This constraint becomes particularly pronounced when communication needs to reflect varying levels of urgency, engagement, or response depth over time. Despite an increasing reliance on natural language interfaces, most chatbot systems remain reactive—responding only to direct input without internal modulation or context-aware initiative [4].

Recent developments in large language models (LLMs) [3], such as ChatGPT, offer a promising solution for platform integration. By enabling communication through natural language, LLM-based interfaces simplify interaction across heterogeneous systems, bypassing the need for rigid APIs or centralized control hubs. However, while LLMs improve interoperability and usability, they do not inherently address the problem of communication regulation within multi-agent networks. Dialogue remains reactive and externally driven, lacking an internal mechanism for adjusting output based on sustained engagement or shifting priorities. Thus, a higher-level control structure is still needed to modulate agent behavior contextually.

In human networks, internal emotional states often govern how individuals initiate, sustain, or inhibit communication. These states evolve in response to both external input and internal regulation, enabling humans to adapt their behavior fluidly across social contexts [5] [7]. Inspired by this mechanism, the proposed framework introduces emotion as an intermediate control layer in artificial agents. Rather than mapping input metrics—such as message frequency, delay, or length—directly to output, incoming signals are first encoded into abstract emotional states. These states evolve continuously over time through analog circuit [8] [9] [10] dynamics such as accumulation, decay, and mutual influence. Output behavior is then generated in response to these internal states, allowing agents to modulate their actions based on internal readiness or inhibition. This emotion-driven structure simplifies coordination, enhances interpretability, and supports adaptive, context-sensitive communication. The framework is validated through simulations in which two agents—alternating between active and passive roles—demonstrate how emotional dynamics shape message behavior and internal regulation over time.

II. Model Design

This section presents the computational framework of the agent's emotional system, illustrated in Figure 1, which is structured into four interconnected modules: *External Input*, *Sensory Processing*, *Internal Emotional State Modeling*, and *External Output*. These components form a closed-loop architecture that continuously transforms external communication stimuli into internal emotional states, which in turn drive adaptive behavioral expressions. The figure outlines the information flow between modules, emphasizing how emotion acts as an intermediary layer between perception and action.

The framework operates by first interpreting environmental signals X_i, where each X_i represents a normalized and encoded feature derived from raw communication input. These signals are routed through a set of temporal filters $F(X)$ in the sensory processing stage, producing processed stimuli Z. The filtered outputs Z drive changes in internal emotional states S, which evolve continuously over time based on both external stimuli and internal feedback mechanisms $G(S)$. The resulting emotional states $y = f(S)$ ultimately determine how the agent behaves through observable outputs.

At the heart of the framework lies the *Internal Emotional State Modeling* module, where three primary emotional sig-

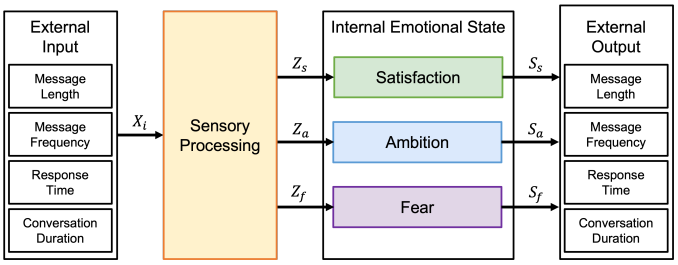

Fig. 1. Overall Framework

nals—**satisfaction**, **ambition**, and **fear**—are maintained as analog voltage states. These emotions interact dynamically to reflect both the agent's current affective experience and its longer-term motivational tendencies.

A. External Input

The External Input module captures raw signals from the agent's communication environment, such as *message length* or *message frequency*. These signals are continuously sampled and normalized into a bounded range to produce stable, comparable values suitable for emotional interpretation. The normalization follows a standard form:

$$\hat{X}(t) = \text{clip}\left(\frac{X(t) - X_{\min}}{X_{\max} - X_{\min} + \varepsilon},\ 0,\ 1\right), \tag{1}$$

where $X(t)$ is the raw input at time t, $X_{\min}$ and $X_{\max}$ define expected feature bounds, and ε prevents division by zero.

Once normalized, each signal is passed through an *Emotion Encoding Function* that transforms it into three emotion-specific analog values: satisfaction, ambition, and fear. These mappings are based on heuristic interpretations of how different input magnitudes influence each emotion—for example, high satisfaction may correlate with longer messages, while fear may rise in response to unusually rapid or large input changes. The output is an emotional stimulus vector:

$$X(t) = \{X_{\text{s}}(t),\ X_{\text{a}}(t),\ X_{\text{f}}(t)\},$$

which represents the raw emotional relevance of the external environment and serves as input to the subsequent *Sensory Processing* module.

B. Sensory Processing

The Sensory Processing module is responsible for converting raw external input signals—such as message length or frequency—into structured, emotion-specific stimuli [11]. These raw inputs are first normalized and mapped to corresponding emotional channels, resulting in intermediate signals $X = \{X_{\text{s}}, X_{\text{a}}, X_{\text{f}}\}$, where each X_i represents the perceptual input related to satisfaction, ambition, or fear. To capture both the persistent intensity and transient dynamics of these signals [6], the module applies a dual-pathway structure consisting of tonic and phasic receptors. These pathways operate in parallel to extract complementary temporal features, ultimately producing the processed outputs $Z = \{Z_{\text{s}}, Z_{\text{a}}, Z_{\text{f}}\}$, which drive changes in the agent's emotional state. The circuit implementation of this dual-pathway architecture is illustrated in Figure 2.

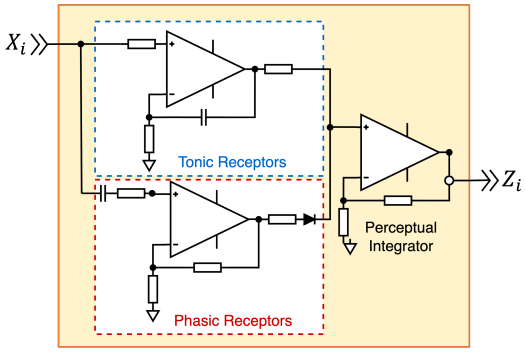

Fig. 2. Sensory Processing Circuit: each input X_i is filtered to produce a time-sensitive output Z_i.

- **Tonic Receptors** simulate the system's sustained attention to environmental input. In the circuit model, they are implemented as *low-pass filters* using summing integrator op-amp circuits. These circuits allow continuous accumulation of input over time, producing outputs that rise gradually with sustained input and decay slowly when input ceases. Mathematically, this behavior can be expressed as a first-order low-pass filter:

$$U_i^{\text{slow}}(t) = \frac{1}{\tau_i}\int_0^t \left(X_i(\tau) - U_i^{\text{slow}}(\tau)\right) d\tau, \tag{2}$$

  where τ_i is the tonic time constant controlling the rate of integration and decay.
- **Phasic Receptors** are responsible for detecting rapid transitions in the input signal. They are realized in the circuit as *high-pass filters*, specifically using leaky differentiator op-amp configurations. These circuits produce sharp, transient outputs in response to sudden increases or decreases in input and decay rapidly to baseline. Their dynamic behavior is captured by the high-pass filter equation:

$$U_i^{\text{fast}}(t) = \tau_d \frac{dX_i(t)}{dt} - U_i^{\text{fast}}(t), \tag{3}$$

  where τ_d is the phasic time constant that controls the responsiveness to fast changes.
  To ensure biologically plausible, excitatory-only responses, the phasic signal is passed through a rectifier circuit that clips negative values. This operation can be modeled mathematically as:

$$\hat{U}_i^{\text{fast}}(t) = \max\left(0, U_i^{\text{fast}}(t)\right). \tag{4}$$

  The rectifier mimics neural mechanisms that primarily transmit excitatory transients while suppressing inhibitory or negative responses.

Finally, the tonic and rectified phasic signals are combined using a weighted summation, forming the final processed signal:

$$Z_i(t) = w_{\text{slow}} \cdot U_i^{\text{slow}}(t) + w_{\text{fast}} \cdot \hat{U}_i^{\text{fast}}(t), \tag{5}$$

where w_{slow} and w_{fast} are tunable weights that determine the influence of tonic and phasic pathways. This fused signal $Z_i(t)$ encodes both the sustained intensity and temporal dynamics of the stimulus, ensuring temporally aware emotional reactions—capturing both how strong and how suddenly a stimulus occurs.

C. Internal Emotional State Modeling

The Internal Emotional State Modeling module governs the evolution of emotional states S based on the filtered stimuli Z. Each emotional variable—*satisfaction* (S_s), *ambition* (S_a), and *fear* (S_f)—is implemented as an analog signal in an independent circuit, and each evolves continuously according to its input and internal feedback. The structure of these emotional circuits, including inter-emotional connections and analog implementations, is shown in Figure 3.

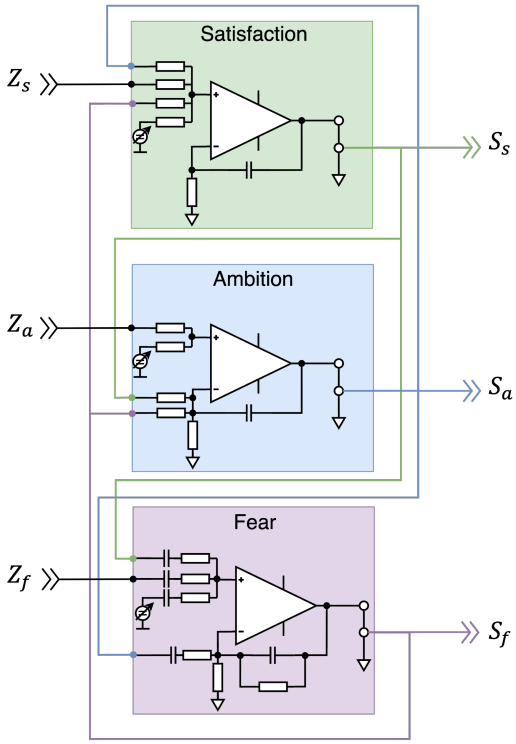

Fig. 3. Emotion Circuit

Satisfaction and **ambition** are realized using summing integrator circuits, which accumulate their respective input signals Z_s and Z_a over time. Their voltage dynamics follow:

$$\frac{dS_i(t)}{dt} = \frac{1}{C_i}\left(-\sum_j \frac{Z_j(t)}{R_{ij}}\right) + G_i(S), \tag{6}$$

where $S_i \in \{S_\text{s}, S_\text{a}\}$, C_i is the integrator capacitor for emotion i, R_{ij} is the resistance from input Z_j, and $G_i(S)$ represents inter-emotional feedback.

Fear, in contrast, is modeled using a leaky differentiator circuit. It reacts sharply to sudden input changes in Z_f, with its output governed by:

$$S_\text{f}(t) = \alpha S_\text{f}(t-1) + \sum_k \frac{C_k}{R_k}\left(Z_k(t) - Z_k(t-1)\right), \tag{7}$$

where $\alpha = e^{-dt/(R_f C_f)}$ is the exponential decay factor, and C_k, R_k are the differentiator's capacitors and resistors for each input Z_k.

The emotional system is further modulated by inter-emotional feedback terms $G(S)$, where outputs from one emotion affect others. For example:

- An increase in fear S_f may suppress ambition: $G_\text{a}(S) = -k_1 S_\text{f}(t)$
- A drop in satisfaction S_s may increase ambition: $G_\text{a}(S) = k_2(1 - S_\text{s}(t))$

The final internal emotional state vector $y = f(S)$ captures the momentary affective configuration of the agent and serves as the basis for behavioral output modulation.

D. External Output

The External Output module translates the internal emotional state vector $y = \{y_\text{s}, y_\text{a}, y_\text{f}\}$ into a single behavioral parameter: *message length*. This parameter represents the richness or expressiveness of the agent's communication and is shaped by the interaction of emotional drives.

Message length is computed as a weighted linear combination of the internal emotional states:

$$L_\text{msg} = w_0 + w_\text{s} \cdot y_\text{s} + w_\text{a} \cdot y_\text{a} + w_\text{f} \cdot y_\text{f}, \tag{8}$$

where w_0 is the baseline message length, and $w_\text{s}, w_\text{a}, w_\text{f}$ are weights associated with satisfaction, ambition, and fear, respectively. These coefficients are selected to reflect behavioral tendencies—for example:

- High **ambition** increases message length.
- High **fear** suppresses message length.
- **Satisfaction** may either reduce or slightly regulate length based on contentment.

To ensure behavioral realism, the final output is clipped to a valid operational range (e.g., $L_\text{msg} \in [0, 100]$):

$$L_\text{msg}^\text{final} = \text{clip}(L_\text{msg},\ 0,\ 100). \tag{9}$$

This output signal defines how much information the agent expresses in a single message and serves as the primary behavioral channel for emotional expression in the current model.

III. Experiments and Results

This section presents simulation-based experiments conducted to evaluate the effectiveness and dynamics of the proposed emotion-driven communication framework. The experiments are divided into progressive layers of analysis, ranging from subsystem validation to full-agent interaction in a communication loop.

A. Experiment Setup

The experimental design is structured around three core modules:

1) **Sensory Processing:** Tests how raw environmental stimuli (e.g., message length) are encoded into emotional signals using the dual-pathway sensory architecture (tonic and phasic circuits).
2) **Internal Emotional Circuits:** Simulates how satisfaction, ambition, and fear evolve over time when stimulated individually. It also examines how inter-emotional feedback shapes internal dynamics, such as inhibition and compensation.
3) **Emotion-Driven Communication:** Integrates all modules into a two-agent interaction framework, where one agent is designated as active and the other as passive in alternating time windows. Agents exchange emotional signals through generated message lengths to evaluate behavioral influence and internal adaptation.

In the communication simulation, roles are pre-assigned and manually switched halfway through the experiment. That is, the role switch is not triggered autonomously by agent behavior but defined explicitly in the simulation configuration.

B. Results

1) Sensory Processing Output: Figure 4 shows how a normalized message-length signal is converted into an emotion-specific stimulus through the sensory processing pipeline. Three distinct phases—spike, adaptation, and decay—are clearly visible, confirming that the dual-pathway processing captures both immediate and sustained components of the signal.

Three characteristic phases emerge in the processed signal:

- **Spike:** A sharp and brief increase at the onset of stimulation, primarily generated by the phasic receptor (modeled as a differentiator). This mirrors biological phasic receptors in humans, such as those found in mechanoreception, which are known to respond quickly to changes but not to constant stimuli.
- **Adaptation:** A gradual rise during the sustained stimulus interval, governed by the tonic receptor's low-pass behavior. The system maintains a smoothed signal while suppressing transient fluctuations. This behavior is comparable to slowly adapting sensory receptors, which continue to respond as long as the stimulus is present but with reduced sensitivity over time.
- **Decay:** After the input returns to zero, the signal drops gradually rather than instantly. This is consistent with the discharge behavior of capacitive integrators and reflects how biological systems slowly return to homeostasis following stimulation.

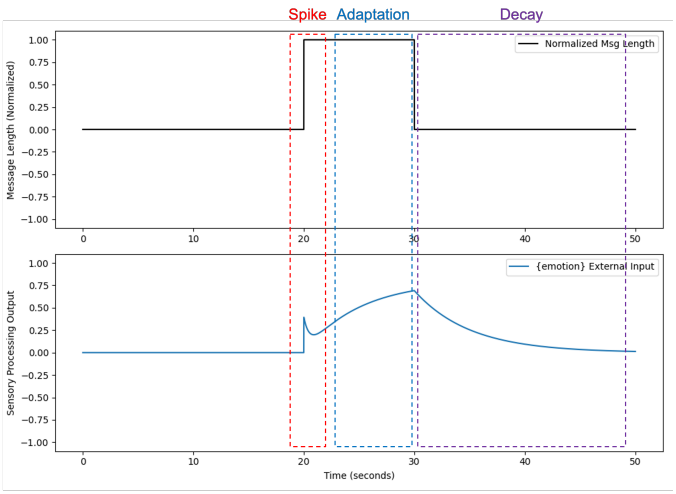

Fig. 4. Sensory processing response to message-length stimulus. Three distinct temporal phases are marked: spike (rapid onset), adaptation (plateau during sustained input), and decay (exponential return to baseline).

From the observation, the combined signal reflects both immediate reactivity and ongoing awareness, capturing the dual nature of human sensory experience: rapid detection followed by gradual internalization and recovery. The shape of the response highlights a dynamic balance between temporal sensitivity (via phasic channels) and cumulative assessment (via tonic channels), aligning with how the human nervous system modulates attention and emotional readiness in response to environmental changes.

2) Internal Emotional Circuit Response: To evaluate the intrinsic behavior of each emotional circuit independently, this section presents controlled stimulation scenarios in which external emotional inputs are directly injected. The aim is to examine how satisfaction, ambition, and fear respond in isolation and interact through feedback mechanisms.

In Figure 5, a sudden drop in external satisfaction input induces a gradual decay in the satisfaction voltage. In response, the ambition circuit shows a compensatory increase due to the absence of positive feedback from satisfaction. The fear signal remains steady, as it is unaffected in this specific case. This behavior reflects the motivational interplay between satisfaction and ambition, where lower fulfillment can provoke increased goal-seeking drive.

Figure 6 depicts the effects of a fear spike. The fear circuit immediately reacts with a sharp transient peak, characteristic of differentiator dynamics. As fear increases, both satisfaction and ambition decrease, demonstrating inhibitory interconnections. This pattern is consistent with emotion theories where fear overrides exploratory or goal-driven behavior, prioritizing inhibition and caution.

Together, these simulations validate the theoretical design of the emotional circuits, confirming that their output aligns with

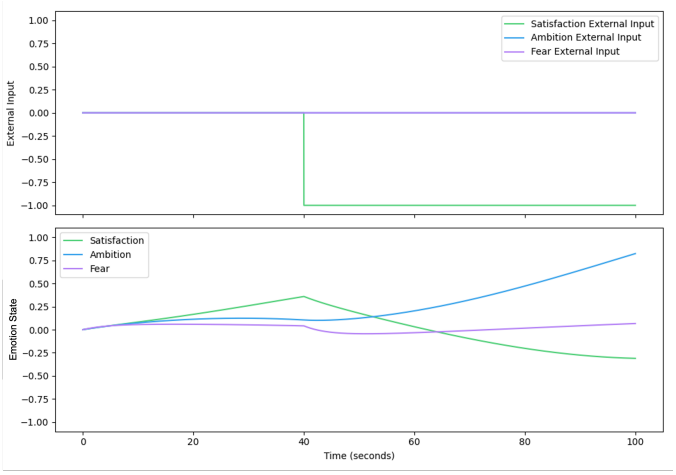

Fig. 5. Response to a decrease in satisfaction input at $t = 40$. Ambition rises gradually as satisfaction decays, and fear remains neutral.

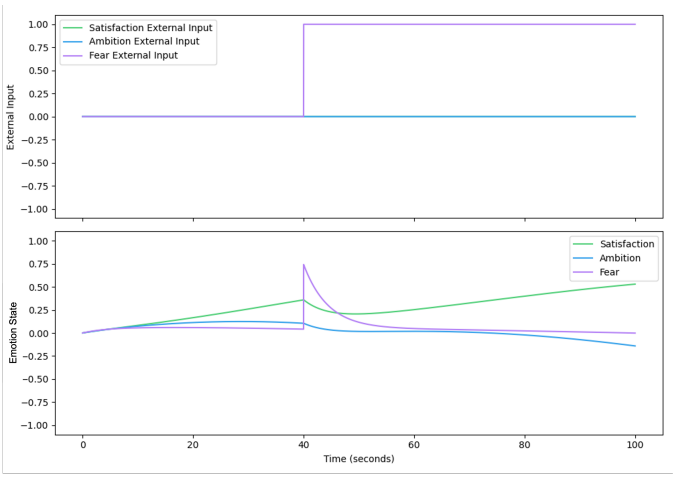

Fig. 6. Response to a spike in fear input at $t = 40$. The fear circuit exhibits a sharp peak followed by decay. Satisfaction and ambition are both suppressed.

both the intended analog behavior and psychological intuition.

3) Emotion-Driven Agent Communication: Figure 7 presents the results from the two-agent simulation. The agents alternate roles in two fixed phases:

1) **Phase 1 (0–50s):** Agent 1 is active and generates message outputs based on its internal emotional state. Agent 2 remains passive and only receives input.
2) **Phase 2 (50–100s):** Agent 2 becomes active while Agent 1 switches to passive mode.

During the first phase (0–50s), Agent 1 is active and generates message-length output modulated by its internal emotional state. At the start, ambition (S_a) is slightly elevated, initiating moderate message production. As the phase progresses, ambition gradually decreases, leading to a corresponding decline in message length. Satisfaction (S_s) remains relatively low due to the lack of incoming input, while fear (S_f) stays minimal. Meanwhile, Agent 2—acting as the passive recipient—receives the message stream as external input.

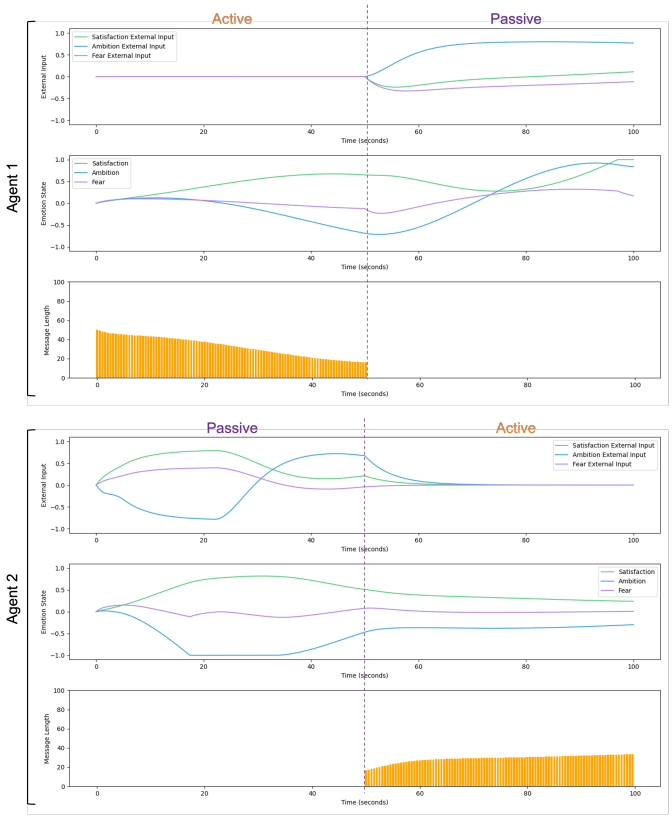

Fig. 7. Bidirectional simulation of emotion-driven agent communication. Top: External inputs, emotional states, and message length output of Agent 1. Bottom: External inputs, emotional states, and message length output of Agent 2.

These signals are processed through tonic and phasic sensory pathways, resulting in a gradual increase in satisfaction and a mild rise in fear in response to sustained stimulation. Ambition in Agent 2 decreases over time, following the increase in satisfaction due to inverse emotional coupling.

At the 50-second mark, roles reverse: Agent 2 becomes active, and Agent 1 becomes passive. A similar emotional pattern unfolds. Agent 2 begins with low ambition and produces moderate-length messages, but as ambition continues to decrease, message length steadily drops. Agent 1, now receiving messages, shows a delayed increase in satisfaction through tonic accumulation, and a moderate rise in fear due to continuous stimulation. Its ambition also decreases as satisfaction builds, replicating the emotional progression seen earlier in Agent 2.

Across both phases, no sharp spikes in fear are observed. This is attributed to the smooth, uninterrupted nature of the input signals—there are no sudden onsets or cessations that would trigger transient phasic fear responses. As a result, fear remains stable and subdued throughout the simulation, while satisfaction and ambition exhibit gradual, inversely coupled trends.

The simulation reveals a consistent emotional-behavioral loop: active agents begin output with low ambition, which

decreases further as messages are emitted. Message length follows this decline closely, reflecting the influence of ambition on output intensity. Passive agents, on the other hand, accumulate satisfaction in response to received messages, which in turn suppresses ambition. Fear rises modestly in both agents but remains stable due to the absence of abrupt emotional stimuli.

This interaction results in:

- Emotion-dependent message generation that self-adjusts based on internal ambition.
- A consistent inverse dynamic between satisfaction and ambition within each agent.
- Emotional adaptation in passive agents driven by external input, even without active participation.
- Smooth transitions supported by the tonic-phasic design, enabling both stability and sensitivity to changes.

Although the switch between active and passive roles is externally configured, the simulation demonstrates how internal emotional states evolve naturally based on message flow. This structure provides a foundation for future implementations where role transitions may be driven autonomously by emotional thresholds or interaction dynamics.

IV. Conclusion

This paper presented an analog emotion-based framework for AI agents, incorporating biologically inspired sensory processing and internal emotional dynamics to modulate communication behavior. Simulations showed that the emotional states—satisfaction, ambition, and fear—respond appropriately to input stimuli, and that these states influence message generation in a continuous and interpretable manner.

In the current setup, however, agents follow predefined active and passive roles to facilitate controlled observation, rather than exhibiting emergent behaviors such as autonomous turn-taking. Moreover, each agent's emotional state is treated as internally driven, responding only to external message stimuli without recognizing or adapting to the emotional state of the other agent. As a result, true emotional interdependence—where one agent's emotional state influences the other's message generation in a feedback loop—is absent.

Future development should address this limitation by integrating mutual emotional awareness. This would allow agents not only to react to message patterns, but to sense and respond to the emotional states of others, enabling richer, more socially intelligent interactions in multi-agent systems.

References

[1] T. Chen, Z. Liu, J. Tang, et al., "AgentVerse: Facilitating Multi-Agent Collaboration through Large Language Models," arXiv preprint arXiv:2210.02199, 2022.

[2] T. Guo, X. Chen, Y. Wang, R. Chang, S. Pei, N. Chawla, O. Wiest, and X. Zhang, "Large Language Model Based Multi-agents: A Survey of Progress and Challenges," in *Proc. Int. Joint Conf. Artif. Intell. (IJCAI)*, Aug. 2024, pp. 8048–8057. doi: 10.24963/ijcai.2024/890.

[3] W. X. Zhao, K. Zhou, J. Li, T. Tang, X. Wang, Y. Hou, Y. Min, B. Zhang, J. Zhang, Z. Dong, Y. Du, C. Yang, Y. Chen, Z. Chen, J. Jiang, R. Ren, Y. Li, X. Tang, Z. Liu, P. Liu, J.-Y. Nie, and J.-R. Wen, "A survey of large language models," *arXiv preprint arXiv:2303.18223*, 2025.

[4] A. Ho, J. Hancock, and A. Miner, "Psychological, relational, and emotional effects of self-disclosure after conversations with a chatbot," *Journal of Communication*, vol. 68, no. 4, pp. 712–733, 2018.

[5] A. Moors, P. Ellsworth, K. Scherer, and N. Frijda, "Appraisal theories of emotion: State of the art and future development," *Emotion Review*, vol. 5, no. 2, pp. 119–124, 2013.

[6] I. Dozmorov and D. Dresser, "Immune system as a sensory system," *Int. J. Biomed. Sci.*, vol. 6, no. 3, pp. 167–175, 2011.

[7] M. R. Roxo, P. R. Franceschini, C. Zubaran, F. D. Kleber, and J. W. Sander, "The limbic system conception and its historical evolution," *Scientific World Journal*, vol. 11, pp. 2428–2441, Dec. 2011.

[8] J. Sun, P. Gao, P. Liu, and Y. Wang, "Memristor-based emotion regulation circuit and its application in faulty robot monitoring," *IEEE Internet of Things Journal*, vol. 11, no. 19, pp. 31633–31645, Oct. 1, 2024.

[9] J. Sun, Y. Zhai, P. Liu, and Y. Wang, "Memristor-based neural network circuit of associative memory with overshadowing and emotion congruent effect," *IEEE Transactions on Neural Networks and Learning Systems*, vol. 36, no. 2, pp. 3618–3630, Feb. 2025.

[10] M. Zhang, C. Wang, Y. Sun, and T. Li, "Memristive PAD three-dimensional emotion generation system based on D–S evidence theory," *Nonlinear Dynamics*, vol. 112, pp. 1–21, 2024.

[11] D. Julius and J. Nathans, "Signaling by sensory receptors," *Cold Spring Harbor Perspectives in Biology*, vol. 4, no. 1, p. a005991, Jan. 2012.